Indonesian Journal of Physics
Vol. 33. No.1, 17 October 2022

Journal homepage: http://ijphysics.fi.itb.ac.id

Thin-shell Solution of Chameleon Mechanism in Brans-Dicke Scalar-Tensor Model

Azwar Sutiono[1,2]*, Agustina Widiyani[2,3], Marliana[2], Getbogi Hikmawan[2,4], Agus Suroso[2,4], Freddy P. Zen[2,4]

[1]*Department of Physics, Faculty of Mathematics and Natural Sciences, Universitas Hasanuddin, Jl. Perintis Kemerdekaan KM. 10 Makassar 90245, Indonesia*
[2]*Theoretical Physics Laboratory, THEPI Division, Department of Physics, Faculty of Mathematics and Natural Sciences, Institut Teknologi Bandung, Jl. Ganesha 10 Bandung 40132, Indonesia*
[3]*Department of Physics, Faculty of Science, Intitut Teknologi Sumatera, Jl. Terusan Ryacudu, Jati Agung Lampung Selatan 35364, Indonesia*
[4]*Indonesia Center for Theoretical and Mathematical Physics (ICTMP) Faculty of Mathematics and Natural Sciences, Institut Teknologi Bandung, Jl. Ganesha 10 Bandung 40132, Indonesia*

(Received: 28 February 2022, Revised: 30 May 2022, Accepted: 11 October 2022)

Abstract

We investigated the chameleon screening mechanism in Brans-Dicke scalar-tensor theory. We preserved the fundamental premise of the typical chameleon mechanism, which is that the field is huge in high-density environments but essentially free in low-density environments like the solar system. We discovered thin-shell solutions for a static and spherical symmetric body and demonstrated the model's applicability to local data.

Keywords: Chameleon, Screening mechanism, Brans-Dicke.

INTRODUCTION

The observation that the universe is expanding accelerated has caused one of the most signifi- cant modern cosmology problems. Recent cosmological data show that the universe comprises about $(22{,}7 \pm 1{,}4)\%$ nonbaryonic dark matter, $4{,}56 \pm 0{,}16)\%$ baryon and $(72{,}8 \pm 0{,}5)$ dark energy (DE) that DE has negative pressure, and explains the current cosmic acceleration. High- precision observational data regarding type Ia supernovae [1,2,3], cosmic microwave background anisotropy [4], and universe age probes [5] prove this acceleration very strongly. This is also confirmed by recent WMAP data [5,10].

One of the challenges in the universe's accelerated expansion by modifying gravity, as we can see from various examples of modified gravity models, is that GR is being tested with remark- able precision in the Solar System. In the quintessence model, the scalar field must assume that its interactions with matter must be set to a small value to satisfy the equivalence principle (EP).In this way, we want an instrument that can mask gravity modification on a limited scale. This technique is known as the screening mechanism. Because the additional degrees of free- dom, which are frequently represented by scalar fields, follow a nonlinear equation (11) that is dependent on density, the screening mechanism occurs. In our cosmos, densities vary in many orders. The universe's critical density is given by $\rho_c = 10^{-29}\ \mathrm{g/cm^3}$. $\rho_{gal} = 10^{-24}\ \mathrm{g/cm^3}$ is the average density inside galaxies. $\rho_{sun} = 10\ \mathrm{g/cm^3}$ represents the density of the Sun. The screen- ing mechanism shifts the behavior of scalar fields driven by density differences from cosmology to the solar system.

Khoury and Weltman [6,7] have introduced a screening mechanism called the chameleon mechanism in the Einstein frame. The mass of the scalar field is not constant in time and space in this mechanism, but rather varies on the density of the local matter.The scalar field's mass is substantial enough to meet the equivalence principle and fifth

* Corresponding author.

E-mail address: azwarsu@gmail.com

force constraints in high density locations, such as on Earth. Of a huge scale, such as the cosmological scale, when matter density is 10^{30} times lower than the local environment, the mass of the scalar field can be on the order of H_0, where H_0 is the current Hubble constant.The scalar field can operate as dark energy to accelerate the universe in this situation. As a simple kind of scalar field, the quintessence, as cosmological scalar fields, has not been detected in EP's local test because we do the test in a dense region. Because scalar fields can hide from our observations and experiments, we call them chameleons [8,13].

There is one aspect of the Chameleon mechanism that has not been explored clearly. Almost all recent works on the chameleon mechanism, namely [6,7,8,13], described the mechanism in the Einstein Frame (EF), in which the chameleon field minimally coupled to curvature scalar [15]. In this paper, we investigated the Chameleon screening mechanism in the Jordan frame (JF), in the form of the Brans-Dicke (BD) scalar-tensor model. The scalar field and geometry already have a nonminimal coupling in BD theory. A nonminimal coupling of the scalar field with the matter sector is added to the action [9,14]. Previously, the Chameleon BD model has been tested, which shows that some potential forms and coupling functions of specific scalar fields do not meet testing on a small scale [11]. A review of post-Newtonian parameters has also been carried out within the framework of the BD Chameleon model [12]. In his review, a scalar field function, which is indicated as a matter-scalar field coupling, was introduced to validate the solar system's constraints. However, it has not explicitly demonstrated the solution of the BD Chameleon field.The basic idea that we did in this work is to keep the original view of the standard chameleon screening mechanism that the scalar field is affected by the den- sity of matter in the environment, and the solution of the BD Chameleon field is shown explicitly.

The following is a breakdown of the paper's structure. The model's ingredients are listed in section 2. In part 3, we look at the model's static, spherical symmetric solution. In part 4, we demonstrate how to test the earth's chameleon field. The final section is devoted to the conclusion.

THE SETUP OF THE MODEL

The Chameleon mechanism of Brans-Dicke's scalar-tensor theory is investigated in this study [9]. Brans-Dicke scalar-tensor action is given by

$$S = \int d^4x\sqrt{-g}\left[\phi R - \frac{\omega_{BD}}{\phi}(\partial\phi)^2 - 2V(\phi)\right] \qquad (1)$$

where $(\partial\phi)^2 = g^{\mu\nu}\partial_\mu\phi\partial_\nu\phi$, $V(\phi)$ is the scalar field self-inteaction potential, w_{BD} is the BD dimensionless coupling parameter, $g_{\mu\nu}$ is the metric in JF and $\tilde{g}_{\mu\nu} = A^2(\phi)g_{\mu\nu}$ is the metric in EF. The equation of motion for ϕ is obtained by varying action (1) with regard to ϕ. We get the equation of motion by requiring $\delta S = 0$,

$$\mathcal{R} + 2\omega_{BD}\left(\frac{\partial\phi}{\phi}\right)^2 - 2V_{,\phi} - 2A_{,\phi}\rho = 0 \qquad (2)$$

We get scalar Ricci R from trace of $G_{\mu\nu}$ from the variation of action (1) respect to $g_{\mu\nu}$,

$$G_{\mu\nu} = \mathcal{R}_{\mu\nu} - \frac{1}{2}g_{\mu\nu}\mathcal{R}$$

$$= \omega_{BD}\left[\frac{\partial_\mu\phi}{\phi}\frac{\partial_\nu\phi}{\phi} - \frac{1}{2}g_{\mu\nu}\left(\frac{\partial\phi}{\phi}\right)^2\right] - g_{\mu\nu}\frac{V}{\phi} + \frac{1}{\phi}\left(\nabla_\mu\nabla_\nu - g_{\mu\nu}\nabla^2\right)\phi + \frac{T_{\mu\nu}}{\phi} \qquad (3)$$

The trace of (3) give

$$\mathcal{R} = \omega_{BD}\left(\frac{\partial\phi}{\phi}\right)^2 + \frac{4V}{\phi} + 3\frac{\nabla^2\phi}{\phi} - \frac{\rho}{\phi} \qquad (4)$$

Substitute (4) to (2) we get the equation of motion,

$$\nabla^2\phi = \frac{2}{3+\omega_{BD}}\left[\phi V_{,\phi} - 2V + \left(A_{,\phi}\phi - \frac{1}{2}\right)\rho\right] \qquad (5)$$

We can express equation (5) in terms of single effective potential

$$\nabla^2\phi = V_{eff,\phi} \qquad (6)$$

where,

$$V_{eff,\phi} = \frac{2}{3+\omega_{BD}}\left[\phi V_{,\phi} - 2V + \left(A_{,\phi}\phi - \frac{1}{2}\right)\rho\right] \qquad (7)$$

Integrate both side of the equation (7), we find the effective potential

$$V_{eff} = \frac{2}{3+\omega_{BD}}\left[\phi V - 3\int V d\phi - \left(A\phi - \int A d\phi - \frac{1}{2}\phi\right)\rho\right]. \qquad (8)$$

The matter density ρ occurs in the effective potential, which is the key point here. We can create a condition where the force due to the scalar field is veiled in high-density regions by choosing the potential and coupling to matter. Figure I shows a comparison of effective chameleon potential in low-density and high-density settings. The potential's shape is considerably shallower in low- density regions, corresponding to a light scalar that mediates a long-range force. The scalar gets a huge mass in high-density zones, and the force is turned off. Therefore, in [6,7,8], the potential $V(\phi)$ was supposed to be of the runaway type, implying that it decreases monotonically. If we choose the potential $V(\phi)$ the Ratra-Peebels potentials and coupling matter $A(\phi)$ like in standard chameleon [5],

$$V(\phi) = \frac{M^{4+n}}{\phi^{n}}, \tag{9}$$

And

$$A(\phi) = 1 + \frac{\beta\phi}{M_{pl}} \tag{10}$$

where M is a constant mass, n is positive constant, β is constant coupling, and M_{pl} is planck Mass, we get

$$V_{eff,\phi} = \frac{2}{3+\omega_{BD}}\left[-(n+2)\frac{M^{4+n}}{\phi^{n}} + \left(\frac{\beta\phi}{M_{pl}} - \frac{1}{2}\right)\rho\right]. \tag{11}$$

The minimum ϕ_{min} of the effective potential is given by the equation

$$V_{eff,\phi} = 0. \tag{12}$$

The effective potential's second derivative is used to calculate the mass associated with the field. ϕ_{min} is used to represent small fluctuations around a minimum, we find

$$m_{eff}^{2} = \frac{2}{3+\omega_{BD}}\left[n(n+2)\left(\frac{M^{4+n}}{\phi_{min}^{n+1}}\right) + \frac{\beta\rho}{M_{pl}}\right]. \tag{13}$$

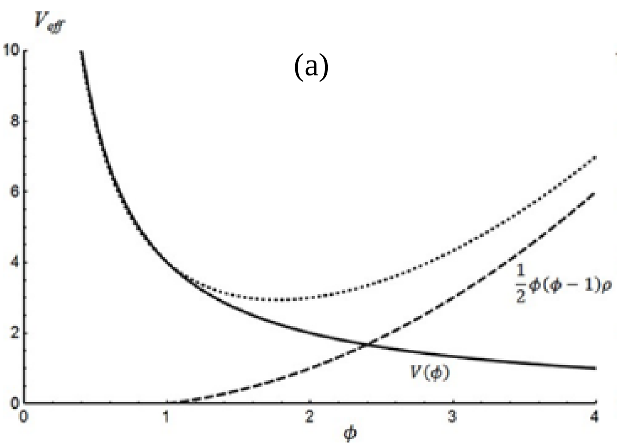

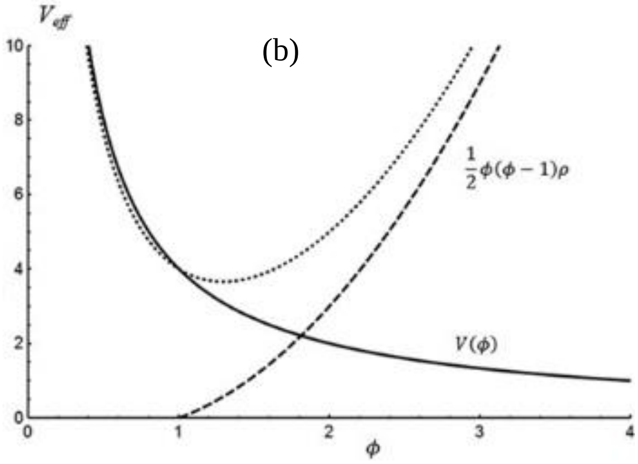

Fig 1. With units and constants removed, a basic example demonstrating the behavior of physically important quantities. The effective potential is the sum of runaway form potential $V(\phi) = 1/\phi^{2}$ and density-dependent piece, from coupling to matter $\frac{1}{2}\phi(\phi-1)\rho$. a.) $\rho = 1$ and b.) $\rho = 3$.

SPHERICAL SOLUTION TO THE FIELD EQUATION

Inside and outside a compact object radius R with a spherical body and homogeneous density ρc in a background of homogeneous density ρ_b, we will search for solutions to the field equation [6,7,8].This may be a ball in the atmosphere with $\rho_b = \rho_{atm}$, or a planet with ρ_b equaling the average matter density in the universe/solar system. The equation of motion (5) reduces to in the case of a static and spherically symmetric background,

$$\frac{d^2\phi}{dr^2} + \frac{2}{r}\frac{d\phi}{dr} = \frac{2}{3+\omega_{BD}}\left[\phi V_{,\phi} - 2V + \left(A_{,\phi}\phi - \frac{1}{2}\right)\rho(r)\right] \tag{14}$$

Where

$$\rho(r) = \begin{cases}\rho_c; & r < R\\ \rho_b; & r > R\end{cases} \tag{15}$$

When discussing quantities defined for the body, the subscript c is used, while when discussing quantities defined for the background, the subscript b is used. ϕ_c is the minimum effective potential inside the body when $\rho = \rho_c$, ρ_b is the minimum in the background where $\rho = \rho_b$, m_c and m_b are the mass of tiny fluctuations around ϕ_c and ϕ_b, respectively. The boundary criteria are imposed by us,

$$\left.\frac{d\phi}{dr}\right|_{r=0} = 0, \quad (16)$$

$$\left.\frac{d\phi}{dr}\right|_{r=\infty} = 0, \quad (17)$$

$$\phi(r \to \infty) = \phi_b, \quad (18)$$

The first condition is based on the symmetry around $r = 0$, whereas the others are based on physical requirements that the ϕ force between a compact object and a test particle diminishes as the distance between them grows infinite.

We will now look for the solution of equation (14) following the scheme in [6]. Equation (14) moves ϕ towards ϕ_c inside the sphere, whereas it drives ϕ towards ϕ_b outside the sphere. To achieve an approximation solution to (14), we will suppose that the driving factor $V_{eff}(\phi)$ can be approximated by a harmonic potential outside the sphere. Then for $r > R$,

$$\frac{d^2\phi}{dr^2} + \frac{2}{r}\frac{d\phi}{dr} = m_b^2(\phi - \phi_b). \quad (19)$$

The general solution of equation (19) is

$$\phi(r) = A\frac{e^{-m_b(r-R)}}{r} + B\frac{e^{m_b(r-R)}}{r} + \phi_b, (20)$$

where A and B are dimensionless constant. Remember the boundary condition that $\phi \to \phi_b$ as $r \to \infty$ gives $B = 0$, so the equation (20) become

$$\phi(r) = A\frac{e^{-m_b(r-R)}}{r} + \phi_b, \quad (21)$$

We will analyze two types of solutions for $r < R$ based on two approximations to equation (14). Define R_c to divide the interval $[0, R_c]$ when $\phi \sim \phi_c$, and $[R_c, R]$ when $\phi \gg \phi_c$. We will get the solution of the equation in each interval on two approximations. The first approximation is when $\phi \gg \phi_c$ that the V_{eff} harmonic approximation is no longer valid. Figure 1 shows that when $\phi > \phi_{min}$, the potential V decays rapidly and the term ρ takes precedence. So, with assuming $\phi \ll M_{pl}$ we can get

$$V_{eff,\phi} \approx \mathcal{M}\left(\frac{\beta\phi}{M_{pl}} - \frac{1}{2}\right)\rho_{c,} \quad (22)$$

Where $\mathcal{W} = \frac{2}{3+\omega_{BD}}$ Equation (14) become

$$\frac{d^2\phi}{dr^2} + \frac{2}{r}\frac{d\phi}{dr} = \mathcal{W}\left(\frac{\beta\phi}{M_{pl}} - \frac{1}{2}\right)\rho_{c.} \quad (23)$$

With the solution in general,

$$\phi(r) = \frac{C}{r}e^{-\sqrt{\frac{\mathcal{W}\beta\rho_c}{M_{pl}}}r} + \frac{D}{2r}\sqrt{\frac{M_{pl}}{M\beta\rho_c}}e^{\sqrt{\frac{\mathcal{W}\beta\rho_c}{M_{pl}}}r} + \frac{M_{pl}}{2\beta}, \quad (24)$$

with C and D are dimensionless constant. The second approximation is when $\phi \sim \phi_c$. In here, The harmonic approximation can be used,

$$V_{eff,\phi} \approx m_c^2(\phi - \phi_c). \quad (25)$$

This time, however, we will write the solution as

$$\phi(r) = E\frac{e^{-m_c r}}{r} + F\frac{e^{m_c(r-R_c)}}{r} + \phi_c, \quad (26)$$

In this paper, we will find the solution for large compact objects. Inside the object $r \ll R$, the field minimizes V_{eff}, and thus $\phi \approx \phi_c$. This condition happened everywhere inside the object expect inside a thin shell of thickness $\Delta R = R - R_c$ below the surface where the field grows (R_c is the distance between the thin shell and the core of the object). Outside the object, when $r > R$, ϕ tends to ϕ_b. We call this the "thin-shell solution" when $0 < R_c < R$. Thin-shell's case for typical chameleon has been solved, demonstrating that ϕ is approximately constant throughout the body, although fluctuations in φ can occur in a tiny region (the thin-shell) near the body's surface[6]. The solution is divided into three regions. In order $\phi(r)$ itself have a limit as $r \to 0$, we must have $E = -Fe^{m_c R}$. As in the case $R_c = R$, we have $E = -Fe^{m_c R_c}$. Then we get ϕ and $\frac{d\phi}{dr}$:

$$\phi(r)=\begin{cases} F\dfrac{e^{m_c(r-R_c)}-e^{-m_c(r+R_c)}+\phi_c}{r}\,; r\in(0,R_c) \\ \dfrac{C}{r}e^{-\sqrt{\frac{\mathcal{W}\beta\rho_c}{M_{pl}}}r}+\dfrac{D}{2r}\sqrt{\dfrac{M_{pl}}{\mathcal{W}\beta\rho_c}}e^{\sqrt{\frac{\mathcal{W}\beta\rho_c}{M_{pl}}}r}+\dfrac{M_{pl}}{2\beta}\,;\ r\in(R_c,R), \\ A\dfrac{e^{-m_b(r-R)}}{r}+\phi_b\ ;\ r\in(R_c,R) \end{cases} \tag{27}$$

$$\frac{d\phi(r)}{dr}=\begin{cases} F\dfrac{m_c r e^{m_c(r-R_c)}-e^{m_c(r-R_c)}+m_c r e^{m_c(r+R_c)}+e^{-m_c(r+R_c)}}{r^2}\,;\ r\in(0,R_c) \\ \dfrac{e^{-r\sqrt{\frac{\mathcal{W}\beta\rho_c}{M_{pl}}}}}{2r^2}\left(\dfrac{De^{2r\sqrt{\frac{\mathcal{W}\beta\rho_c}{M_{pl}}}}\sqrt{M_{pl}}(-1+r)\sqrt{\dfrac{\mathcal{W}\beta\rho_c}{M_{pl}}}}{\sqrt{\mathcal{W}\beta\rho_c}}-2C\left(1+r\sqrt{\dfrac{\mathcal{W}\beta\rho_c}{M_{pl}}}\right)\right); r\in(R_c,R), \\ A\dfrac{-m_b e^{-m_b(r-R)}-e^{-m_b(r-R)}}{r^2}\,;\ r\in(R,\infty) \end{cases} \tag{28}$$

There are four continuity equations in this scenario, two at R_c,

$$F\frac{1-e^{-2m_cR_c}}{R_c}+\phi_c=\frac{C}{R_C}\,e^{-\sqrt{\frac{\mathcal{W}\beta\rho_c}{M_{pl}}}R_c}+\frac{D}{2R_C}\sqrt{\frac{\mathcal{W}\beta\rho_c}{M_{pl}}}e^{\sqrt{\frac{\mathcal{W}\beta\rho_c}{M_{pl}}}R_c}+\frac{M_{pl}}{2\beta} \tag{29}$$

$$F\frac{m_cR_c-1+m_cR_ce^{-2m_cR_c}+e^{-2m_cR_c}}{R_c^2}=\frac{e^{-R_c\sqrt{\frac{\mathcal{W}\beta\rho_c}{M_{pl}}}}}{2R_c^2}\left(\frac{De^{4R_c\sqrt{\frac{\mathcal{W}\beta\rho_c}{M_{pl}}}}\sqrt{M_{pl}}(-1+R_c)\sqrt{\frac{\mathcal{W}\beta\rho_c}{M_{pl}}}}{\sqrt{\mathcal{W}\beta\rho_c}}-2C\left(1+R_c\sqrt{\frac{\mathcal{W}\beta\rho_c}{M_{pl}}}\right)\right) \tag{30}$$

And two at R

$$\frac{C}{R}e^{-\sqrt{\frac{\mathcal{W}\beta\rho_c}{M_{pl}}}R}+\frac{D}{2R}\sqrt{\frac{M_{pl}}{\mathcal{W}\beta\rho_c}}e^{\sqrt{\frac{\mathcal{W}\beta\rho_c}{M_{pl}}}R}+\frac{M_{pl}}{2\beta}=\frac{A}{r}+\phi_b \tag{31}$$

$$\frac{e^{-R\sqrt{\frac{v\beta\rho_c}{M_{pl}}}}}{2R^2}\left(\frac{De^{2R\sqrt{\frac{\mathcal{W}\beta\rho_c}{M_{pl}}}}\sqrt{M_{pl}}(-1+R)\sqrt{\frac{\mathcal{W}\beta\rho_c}{M_{pl}}}}{\sqrt{\mathcal{W}\beta\rho_c}}-2C\left(1+R\sqrt{\frac{\mathcal{W}\beta\rho_c}{M_{pl}}}\right)\right)=A\frac{-m_bR-1}{R^2} \tag{32}$$

above case, the exterior approximate solution is

$$\phi(r)=A\frac{e^{-m_b(r-R)}}{r}+\phi_b, \tag{33}$$

Khoury and Weltman assume in the thin-shell scenario $\phi=\phi_c$ for $r<R_c$. So it means that $F=0$. Then, we will get continuity equations (29) and (30),

$$\phi_c=\frac{C}{R_c}\,e^{-\sqrt{\frac{\mathcal{W}\beta\rho_c}{M_{pl}}}R_c}+\frac{D}{2r_C}\sqrt{\frac{\mathcal{W}\beta\rho_c}{M_{pl}}}e^{\sqrt{\frac{\mathcal{W}\beta\rho_c}{M_{pl}}}R_c}+\frac{M_{pl}}{2\beta} \tag{34}$$

$$\frac{De^{4R_c\sqrt{\frac{\mathcal{W}\beta\rho_c}{M_{pl}}}}\sqrt{M_{pl}}(-1+R_c)\sqrt{\frac{\mathcal{W}\beta\rho_c}{M_{pl}}}}{\sqrt{\mathcal{W}\beta\rho_c}} = 2C\left(1+R_c\sqrt{\frac{\mathcal{W}\beta\rho_c}{M_{pl}}}\right) \quad (35)$$

And we get

$$C = -\frac{e^{R_c\sqrt{\frac{\mathcal{W}\beta\rho_c}{M_{pl}}}}\sqrt{M_{pl}}R_c(R_c-1)(M_{pl}-2\beta\phi_c)}{2\beta\left(-\sqrt{M_{pl}}+\sqrt{M_{pl}}R_c+\sqrt{\mathcal{W}\beta\rho_c}+R_c\frac{\mathcal{W}\beta\rho_c}{\sqrt{M_{pl}}}\right)} \quad (36)$$

$$D = \frac{e^{R_c\sqrt{\frac{\mathcal{W}\beta\rho_c}{M_{pl}}}}R_c\sqrt{\mathcal{W}\beta\rho_c}\left(1+\sqrt{\frac{\mathcal{W}\beta\rho_c}{M_{pl}}}\right)M_{pl}-2\beta\phi_c}{\beta\sqrt{\frac{\mathcal{W}\beta\rho_c}{M_{pl}}}\left(-\sqrt{M_{pl}}+\sqrt{M_{pl}}R_c+\sqrt{\mathcal{W}\beta\rho_c}+R_c\frac{\mathcal{W}\beta\rho_c}{\sqrt{M_{pl}}}\right)} \quad (37)$$

Substitute equation (36) and (37) into equation (32) with assuming $m_b R \ll 1$,we get

$$A \approx -\frac{e^{-(R_c+R)\sqrt{\frac{\mathcal{W}\beta\rho_c}{M_{pl}}}}(M_{pl}-2\beta)}{2\beta}\left(\frac{e^{R_c\sqrt{\frac{\mathcal{W}\beta\rho_c}{M_{pl}}}}M_{pl}R_c\left(-R_c+\sqrt{\frac{\mathcal{W}\beta\rho_c}{M_{pl}}}\right)\left(1+R\sqrt{\frac{\mathcal{W}\beta\rho_c}{M_{pl}}}\right)}{-R_c(\mathcal{W}\beta\rho_c+M_{pl})+M_{pl}\left(\sqrt{\frac{M_{pl}}{\mathcal{W}\beta\rho_c}}-\sqrt{\frac{\mathcal{W}\beta\rho_c}{M_{pl}}}\right)} + \frac{e^{2R\sqrt{\frac{\mathcal{W}\beta\rho_c}{M_{pl}}}}R_c\left(R+\sqrt{\frac{M_{pl}}{\mathcal{W}\beta\rho_c}}\right)\left(\mathcal{W}R_c\beta\rho_c+\sqrt{\frac{\beta\rho_c}{M_{pl}}}\right)}{\sqrt{\frac{\beta\rho_c}{M_{pl}}}\left(R_c(\mathcal{W}\beta\rho_c-M_{pl})+M_{pl}\left(\sqrt{\frac{M_{pl}}{\mathcal{W}\beta\rho_c}}-\sqrt{\frac{\mathcal{W}\beta\rho_c}{M_{pl}}}\right)\right)}\right). \quad (38)$$

Finally we find the approximate exterior solution of the thin-shell case

$$\phi_{thin}(r) \approx -\frac{e^{-(R_c+R)\sqrt{\frac{\mathcal{W}\beta\rho_c}{M_{pl}}}}(M_{pl}-2\beta)}{2\beta}\left(\frac{e^{R_c\sqrt{\frac{\mathcal{W}\beta\rho_c}{M_{pl}}}}M_{pl}R_c\left(-R_c+\sqrt{\frac{\mathcal{W}\beta\rho_c}{M_{pl}}}\right)\left(1+R\sqrt{\frac{\mathcal{W}\beta\rho_c}{M_{pl}}}\right)}{-R_c(\mathcal{W}\beta\rho_c+M_{pl})+M_{pl}\left(\sqrt{\frac{M_{pl}}{\mathcal{W}\beta\rho_c}}-\sqrt{\frac{\mathcal{W}\beta\rho_c}{M_{pl}}}\right)} + \frac{e^{2R\sqrt{\frac{\mathcal{W}\beta\rho_c}{M_{pl}}}}R_c\left(R+\sqrt{\frac{M_{pl}}{\mathcal{W}\beta\rho_c}}\right)\left(\mathcal{W}R_c\beta\rho_c+\sqrt{\frac{\beta\rho_c}{M_{pl}}}\right)}{\sqrt{\frac{\beta\rho_c}{M_{pl}}}\left(R_c(\mathcal{W}\beta\rho_c-M_{pl})+M_{pl}\left(\sqrt{\frac{M_{pl}}{\mathcal{W}\beta\rho_c}}-\sqrt{\frac{\mathcal{W}\beta\rho_c}{M_{pl}}}\right)\right)}\right)\frac{e^{-m_b(r-R)}}{r}+\phi_b. \quad (39)$$

As we assumed before, R_c is distance between the thin-shell and core of the object that can be found with combine equation (31), (36), (37), and (38).

DETECTING CHAMELEON FIELD FOR THE EARTH

For the earth, we shall present an example of a chameleon field. Let us imagine the Earth as a sphere with radius $R = 6 \times 10^6$ m and density $\rho_c = 10\ \mathrm{g/cm^3}$ surrounded by an interplanetary medium of density $\rho_b = 10^{-24}\,\mathrm{g/cm^3}$. We take the constant $n = 1$, $\beta = 10^{19}$, $\omega_{BD} = 10^{50}$ and $M = 10^{30}\mathrm{GeV}$. First of all, we will find the minimum ϕ_b, ϕ_c and effective mass m_b based on equation (11) and (13). Figure 2 show the plot of BD chameleon field as the function of r. We are able to see that $\phi \approx \phi_c$ everywhere inside the earth, except within $5{,}96 \times 10^6\mathrm{m} \leq r \leq 6 \times 10^6\mathrm{m}$ as the thin shell of the earth.

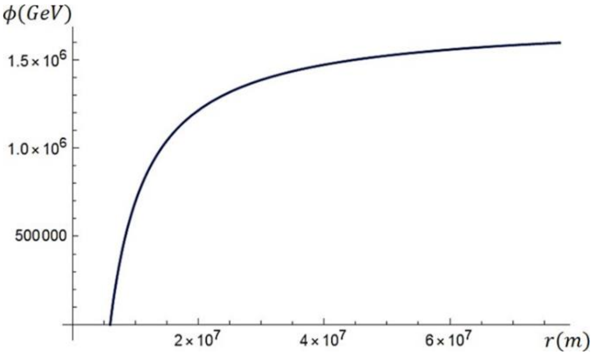

Figure 2. The Earth's Chameleon Field in Brans-Dicke model.

CONCLUSION

In this paper, we have derived a thin-shell solution of a chameleon scalar field ϕ of the BD scalar-tensor model in the background of a spherically symmetric body. The solution is then applied to the earth by selecting the appropriate constants. We can see the chameleon field increase exponentially after it crosses the earth's radius and becomes constant at infinity.The modest magnitude of scalar field obtains a huge mass of chameleon field and turns off the fifth force in high density locations near the earth's surface. A light scalar mediates a long-range force in low density regions far from the earth, bringing up the influence of modified gravity in the cosmological background.

ACKNOWLEDGEMENT
This work was supported by Program Riset dan Inovasi Kelompok Keilmuan ITB 2020.

REFERENCES
[1] A. G. Riess, et. al., Observational Evidence from Supernovae for an Accelerating Universe and a Cosmological Constant, *Astron J.* 116, 1009,1998.
[2] A. G. Riess, et. al., BVRI Light Curves for 22 Type Ia Supernovae, *Astron. J.* 117, 707 , 1999.
[3] S.Perlmutter et. al., Discovery of a Supernova Explosion at Half the Age of the Universe and its Cosmological Implications, *Nature* 391, 51,1998.
[4] M. Hicken et al., *Astrophys. J.* 700, 1097, 2009 [arXiv:0901.4804 [astro-ph].
[5] E. Komatsu et al., Seven-Year Wilkinson Microwave Anisotropy Probe (WMAP) Observations: Cosmological Interpretation, *Astrophys. J. Suppl.* 180, 330, 2009 arXiv : 0803.0547 [astro-ph].
[6] Khoury, J., and Weltman, A., Chameleon cosmology, *Phys. Rev. D* 69, 044026, 2004.
[7] Khoury, J., and Weltman, A., Chameleon Fields: Awaiting Surprises for Tests of Gravity in Space, *Phys.Rev.Lett.* 93 171104, 2004.
[8] Waterhouse, T. P., An Introduction to Chameleon Gravity, 2006[astro-ph/061186].
[9] C. Brans and R. H. Dicke, Mach's Principle and a Relativistic Theory of Gravitation, *Phys. Rev.* 124, 925, 1961
[10] G. Hinshaw et al., Nine-year Wilkinson Microwave Anisotropy Probe (WMAP) Observations: Cosmological Parameter Results, *Astrophys. J. Suppl.*, 208, 19, 2013.
[11] Y. Bisabr, Notes on the Chameleon Brans-Dicke gravity, *Astrophysics and Space Science* 350, 407-411, 2014.
[12] K. Saaidi et al., γ parameter and Solar System constraint in chameleon-Brans-Dicke theory, *Physical Review D*, 83, 104019, 2011.
[13] T. Nakamura et al., Chameleon field in a spherical shell system, *Physical Review D*, 99, 044024, 2019.
[14] J. Lu et al., The generalized Brans-Dicke theory and its cosmology, *Eur. Phys. J. Plus*, 134, 318, 2019.
[15] C. Burrage and J. Sakstein, Tests of chameleon gravity, *Living Rev. Relativity* 21, 1, 2018.